Water Supply

IWA PUBLISHING

Water Supply Vol 22 No 3, 3484 doi: 10.2166/ws.2021.389

Experimental investigation of scouring around a single spur under clear water conditions

Cansu Özyaman [a,*], Cahit Yerdelen [a], Ebru Eris [a] and Rasoul Daneshfaraz [b]

[a] Department of Civil Engineering, Ege University, Izmir 35040, Turkey
[b] Department of Civil Engineering, University of Maragheh, Maragheh, Iran
*Corresponding author. E-mail: cansu.ozyaman@ege.edu.tr

CÖ, 0000-0002-0573-0446; CY, 0000-0003-4705-1940; EE, 0000-0003-0601-7666; RD, 0000-0003-1012-8342

ABSTRACT

This study presents the effect of different parameters on the scouring process around spur dikes. Our research group's stated objective was to evaluate the effects of sediment gradation, flow depth, spur angle and spur length on the scouring process. Since most existing studies generally employed uniform sediment, in this study uniform and non-uniform sediment were selected. Experiments were made in a rectangular open channel in uniform flow conditions. Results showed that the effect of the spur dike length and the orientation angle on sediment scour varies with the type of sediment used. Scour volumes were 40% greater in uniform sediments than in non-uniform sediments. Measured scour depth was maximum at spurs perpendicular to the flow, whereas the scour volume was maximum at spurs directed upstream. The scour depth increased with an increase in the spur length; however, the effect of spur length on scouring varied at a contraction rate of 0.29 for uniform sediments and 0.36 for non-uniform sediments. A multiple regression analysis was also performed, and four equations were suggested to predict the scour depth and scour volume. Comparisons were made with the literature equations applicable for clear-water scouring to check the suggested equation. Because of the wide range of contraction ratios considered in this study, the equations which considered the contraction effect yielded better estimates.

Key words: clear-water scour, open channel flow, spur dike, uniform and non-uniform sediment

HIGHLIGHTS

- In this study in addition to scour depth measurements, we made scour volume measurements and drew contour line maps to observe the scouring area.
- Since the sediments in rivers and natural channels are non-uniform, we performed the experiments with both uniform and non-uniform sediments.
- Based on the experimental results, we propose four different equations to quantify the scour depth and scour volume in uniform and non-uniform sediments.

INTRODUCTION

The prediction of scouring amount around river training structures is an essential problem in rivers due to its importance in river engineering projects. Spur dikes as one of the important river training structures are hydraulic structures that control sediment deposits and reduce bank erosion by deflecting high-velocity flow away from vulnerable riverbanks.

Spur dikes cause flow resistance, resulting in the deformation of flow lines. The deformed flow lines produce vortex systems of different sizes, which initiate and control the scouring process. A primary vortex (the same as the horseshoe vortex observed around bridge piers) is formed around the scour hole at the upstream side of the spur dike. The horseshoe vortex extends downstream of the spur dike or pier and loses its strength before losing its identity and becoming part of the general turbulence (Zhang 2005). The flow detaching from the spur dike accelerates and leads to the development of wake vortices. The wake vortices are directed upward to the free surface and have largely vertical axes (Kirkil *et al.* 2008; Uddin & Rahman 2012; Pandey *et al.* 2017).

Scour formed by the effect of these vortices can comprise local scour and contraction scour. Local scour is defined as sediment removal around any structure that may be encountered in a flow path due to different vortex formations (Chiew 1984). However, contraction scour is due to the reduction in the cross-sectional area of the channel. The contraction of the cross-sectional area increases the flow velocity and bed shear stress (Briaud *et al.* 1999). The contributions of these two scour types are usually estimated separately and then taken together without considering mutual interactions (Melville 1997; Richardson

& Davis 2001). However, these processes occur simultaneously and interact with each other. Ballio & Orsi (2001) indicated that these factors are interconnected and found that their effect on scouring is significant only at extreme values of the contraction ratio (ratio of spur dike length to channel width, b/B). Breusers & Raudkivi (1991) also demonstrated that the contraction ratio has no significant effect on local scour if the ratio is lower than 0.4. Singh *et al.* (2020) investigated the effect of contraction, and they selected contraction ratios between 0.2 and 0.6 to propose equations calculating time-dependent scour depth. In this study, the spur dike length was determined for a contraction rate of 0.4 as suggested by Breusers & Raudkivi (1991). However, the effect of the opposite wall was observed for the contraction ratios of 0.29 and 0.36. Ballio *et al.* (2009) stated that the effect of contraction ratio depends on the median particle size (d_{50}) and flow depth. Therefore, the results of this study should be evaluated in terms of the sediment particle size considered in the present study.

In addition to contraction ratio, spur dike orientation angle is also a significant parameter in the scouring problem. Previous studies have shown that the scour depth increases with a decrease in the spur dike orientation angle (Ahmad 1953; Zaghloul 1983; Melville & Coleman 2000). However, in some studies (Kandasamy 1985; Kwan 1988), the scour depth was found to be maximum at 90° spurs. Zhang *et al.* (2018) indicated that the scour depth and scour volume were maximum when the orientation angle was 90°. Dey *et al.* (2017) studied an experimental channel bend, and found that a 15° vane angle produced minimum scour depth while a 40° spur angle produced maximum scour depth. Clearly, previous results are not entirely consistent and sometimes contradictory. Therefore, when interpreting results related to the orientation angle, the sediment particle size distribution, sediment transport conditions and spur dike geometry are vital.

According to their particle size distribution, sediments are classified into two groups. The geometric standard deviation given by $\sqrt{d_{84}/d_{16}}$ is less than 1.4 for uniform sediments and greater than 1.4 for non-uniform sediments (Dey *et al.* 1995). In non-uniform sediments, the flow can drag fine base materials that mobilise easily but not coarse base materials, in which case armouring occurs. Armouring is a process that decreases scouring, causing base movements and a decrease in the scour volume and depth (Melville & Sutherland 1988). Since the observation of armouring in non-uniform sediments depends on gradation of sediment, the scouring mechanism is more complex in non-uniform sediments.

Depending on the sediment transport conditions, scour can be divided into two types: clear-water scour and live-bed scour. Clear-water scour occurs when the shear stress induced by the water flow exceeds the critical shear stress of the bed material. Generally, in the case of clear-water scour, no refilling occurs because of the lack of suspended sediments. Clear-water scour occurs without any sediment motion on the bed away from the structure when $0.4 < V/V_c < 1$, where V is the mean flow velocity and V_c is the threshold velocity at which sediment movement is initiated. When $V/V_c > 1$, live-bed scour occurs, with sediment transport over the entire bed and the scour hole continuously supplied with sediments via the approaching flow (Yuan *et al.* 2017). In live-bed conditions, the scour depth increases rapidly and, due to the interaction between erosion and deposition, it tends to fluctuate around an equilibrium value (Richardson & Davis 2001). Various studies have been conducted under different scour conditions, including experiments under clear-water conditions (Kuhnle *et al.* 1999, 2002; Ezzeldin *et al.* 2007; Kothyari *et al.* 2007; Gisonni & Hager 2008; Ballio *et al.* 2009; Zhang *et al.* 2009; Pagliara *et al.* 2015; Aksoy *et al.* 2017; Karimi *et al.* 2017; Yılmaz *et al.* 2017; Pandey *et al.* 2018; Bestawy *et al.* 2020). Some researchers have performed experiments under live-bed conditions (Sheppard & Miller 2006), whereas others performed experiments under both conditions (Ahmad 1953; Gill 1972; Melville & Sutherland 1988; Richardson & Davis 2001).

In this study, we present the results of several laboratory experiments conducted on spur dikes. The research goal of this study is to investigate the effects of flow depth, contraction ratio, spur dike orientation angle and sediment uniformity on the spur dikes. Studies on sedimentation have shown that the volume and geometry of erosion are as important as the maximum scour depth amounts. In addition to previous studies on scour depth determination, we present more extensive results including the scour volume and contour line maps of the scouring area. Most existing studies generally employed uniform sediments. Since the sediments in rivers and natural channels are non-uniform, it is important to observe non-uniform sediments and to develop the range of sediment diameter and uniformity. Therefore, we selected both uniform and non-uniform sediments, to determine the effect of uniformity. Based on the experimental results, we propose four different equations to quantify the scour depth and scour volume in uniform and non-uniform sediments.

LABORATORY SETUP AND EXPERIMENTS

The experiments were made to observe scour mechanism of a single spur dike. Experiments were conducted in a glass-sided, tilted, slope-adjustable flume located at the Ege University Hydraulic Laboratory (Figure 1). The flume is 0.7 m wide, 18 m

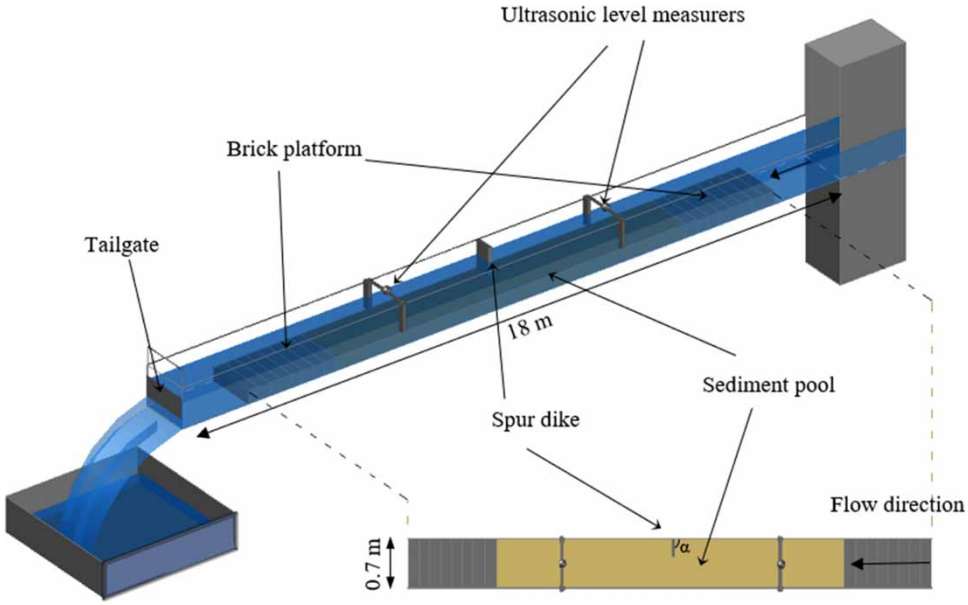

Figure 1 | Experimental channel and plan of spur dike area.

long and 0.5 m deep with a 1.5 m long settling tank located upstream. The longitudinal slope of the flume was fixed at 0.5%. A rectangular cross-sectioned, straight experimental channel was used as recommended in USACE (1989). The laboratory experiments were conducted with comparable dimensions of typical micro-models.

Water was first collected in a settling tank in order to provide uniform flow conditions. For the same purpose, a downstream pool was established, permitting free fall at the end of the channel. To avoid turbulence and initial scour, the tailgate was closed, and the channel was filled with water on both sides at a very low rate until the water level reached 1 m. When the water level reached 1 m, the tailgate was slowly opened, and water flowed into the channel. This allowed a smooth approach before the sediment pool. The tailgate was used to regulate the water depth. A pre-determined flow condition was established using the inlet valve and the tailgate.

An 18.5-cm-high brick platform was placed in the channel to construct a sediment pool above the bottom of the channel. Experiments were carried out by placing aerated concrete spur dikes with different sizes and angles on the right-hand bank of the sediment pool. Spur dikes were placed at angles of $\alpha = 45°$, 90° and 135° with respect to the flow. Spur dike lengths perpendicular to the flow (b) were 15 cm, 20 cm, and 25 cm. The spur dike thickness was set to 5 cm in all the experiments. The spur dike height had no effect on the experimental conditions since unsubmerged spur dikes were used in all the experiments.

All the experiments were performed in steady flow conditions. The experiments were performed under three different discharges (15, 30 and 45 l/s) for the spur dikes angled at 45° and 135°, whereas seven different discharge values (15, 20, 25, 30, 35, 40 and 45 l/s) were used on the 90° spur dikes in order to observe the effect of discharges between 15, 30 and 45 l/s. The discharges were measured using an electromagnetic flow sensor installed on the supply pipe and adjusted with the help of a computer program.

Two ultrasonic level measuring instruments with an accuracy of 0.5 mm were placed both upstream and downstream of the spur dike. Ultrasonic level measuring instruments and flow meter values measured at each second were recorded with the help of the data collector. The mean flow depths were then calculated by averaging the ultrasonic level measurement data for each experiment.

To ensure that flow intensity (V/V_c) is less than 1 (clear-water conditions), the water depths were calculated for each discharge. The water depths were determined at a flow intensity value of 0.45, which was approximately the same for all the experiments. The gate at the end of the channel was adjusted and fixed at a specified level to provide the pre-determined water depths. The experimental conditions are given in Table 1.

Two different base materials were used in the experiments: uniform and non-uniform sediments. These materials were chosen in order to associate the scour depths with sediments having different gradations but similar median grain diameter. Gradations

Table 1 | Experimental conditions (α: spur dike angle, b: spur dike length, Q: discharge, y: mean flow depth, Fr: approach Froude number)

		Non-uniform sediment			Uniform sediment		
α	b (m)	Q (l/s)	y_{mean} (m)	Fr	Q (l/s)	y_{mean} (m)	Fr
135°	0.25	15	0.120	0.167	15	0.11	0.196
135°	0.25	31	0.191	0.167	29	0.19	0.165
135°	0.25	43	0.271	0.140	44	0.27	0.150
135°	0.20	16	0.116	0.186	15	0.11	0.192
135°	0.20	30	0.196	0.155	29	0.19	0.162
135°	0.20	44	0.262	0.150	44	0.26	0.153
135°	0.15	15	0.120	0.220	15	0.12	0.165
135°	0.15	29	0.020	0.147	30	0.19	0.164
135°	0.15	45	0.025	0.162	44	0.26	0.155
90°	0.25	16	0.101	0.221	15	0.10	0.216
90°	0.25	20	0.129	0.194	21	0.12	0.207
90°	0.25	25	0.156	0.183	24	0.16	0.185
90°	0.25	30	0.181	0.180	30	0.18	0.176
90°	0.25	35	0.206	0.172	35	0.20	0.172
90°	0.25	39	0.229	0.164	40	0.23	0.166
90°	0.25	44	0.248	0.161	45	0.26	0.158
90°	0.20	15	0.100	0.209	15	0.10	0.205
90°	0.20	20	0.129	0.198	19	0.13	0.191
90°	0.20	25	0.156	0.186	25	0.16	0.187
90°	0.20	31	0.184	0.177	30	0.19	0.172
90°	0.20	35	0.207	0.168	35	0.21	0.167
90°	0.20	39	0.231	0.161	40	0.24	0.160
90°	0.20	44	0.251	0.160	45	0.25	0.163
90°	0.15	16	0.101	0.224	14	0.11	0.192
90°	0.15	20	0.127	0.201	20	0.14	0.168
90°	0.15	25	0.154	0.186	24	0.16	0.176
90°	0.15	31	0.183	0.179	29	0.19	0.163
90°	0.15	35	0.208	0.168	35	0.21	0.166
90°	0.15	40	0.232	0.163	40	0.24	0.158
90°	0.15	45	0.252	0.160	44	0.26	0.157
45°	0.25	15	0.106	0.203	14	0.12	0.171
45°	0.25	29	0.199	0.146	29	0.19	0.168
45°	0.25	43	0.279	0.133	45	0.26	0.154
45°	0.20	15	0.111	0.188	14	0.11	0.180
45°	0.20	30	0.190	0.166	29	0.20	0.153
45°	0.20	44	0.266	0.146	44	0.27	0.148
45°	0.15	15	0.109	0.189	15	0.11	0.190
45°	0.15	29	0.181	0.180	30	0.19	0.162
45°	0.15	45	0.262	0.147	45	0.27	0.150

of uniform and non-uniform sediments are given in Figure 2. The uniformity coefficients (geometric standard deviation) of the materials were 2.92 and 1.37. The grain diameter of the uniform material was between 1 and 2 mm, whereas that of the non-uniform material was between 0.1 and 3 mm. The median grain diameters (d_{50}) of the non-uniform and uniform sediments were

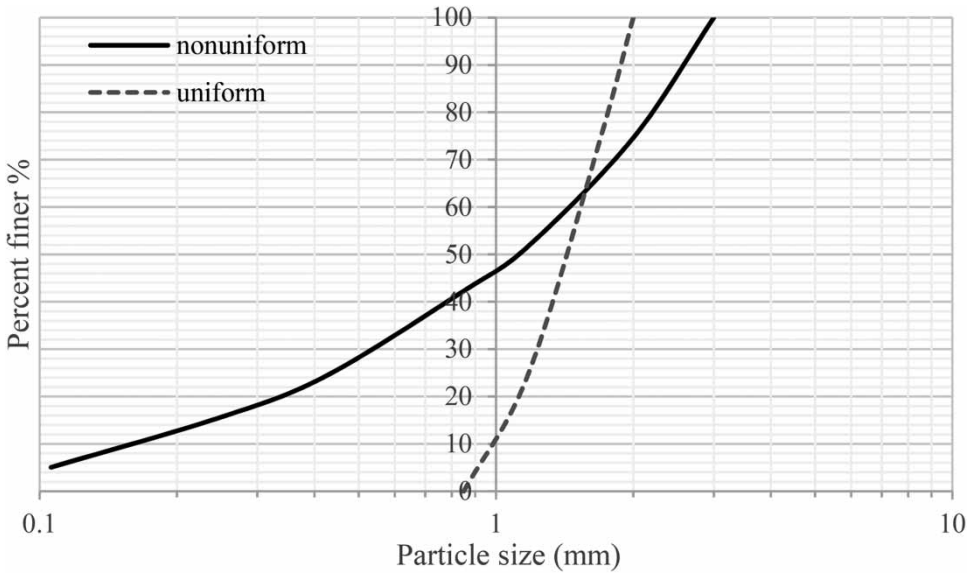

Figure 2 | Gradation of uniform and non-uniform sediment.

approximately 1.12 mm and 1.43 mm, respectively. After the sediment bed was prepared, the recirculating channel was first filled with tap water to an average depth of 18.5 cm. Thereafter the level of saturated sand was carefully straightened. Before all experiments, sediment in the pool was completely mixed to avoid the deposition of coarser sediments at a certain point.

The gate at the end of the channel was completely closed and the channel was filled with water to a certain level before the experiments. Subsequently, by keeping the discharge at a low rate, we opened the gate in a controlled manner until the water level dropped to the required level. Thus, initial scouring was minimised. The experiments started when the desired level and discharge were obtained and ended when the rate of scour depth change was negligible. It should be noted here that the aim of this study was not to determine the equilibrium time for the scour depth. The water in the channel was emptied on both sides at a very low speed (approximately 1 l/s) to prevent scouring after finishing the experiment.

A digital laser meter was used to measure the scour depths. To determine the scour volumes, 5×5 cm axes were constructed on the scouring area. Scour depth coordinates were measured at more than 500 points after completely draining the water in the channel. A 3D scour map was plotted, and the scour volume was calculated from the measurements via a computer program.

RESULTS AND DISCUSSION

The results of more than 50 experiments performed under clear-water conditions showed that local scour was affected by the following variables.

Effect of gradation

In almost all the experiments with the non-uniform base material, the difference in the particle sizes caused armouring around the spur dikes. The results showed that the scour amount with the non-uniform sediments was less than that with the uniform sediments, consistent with previous studies. Since the particle size difference was less in uniform sediments, the flow mobilised all the particles simultaneously and armouring did not occur. Consequently, the scour volume and scour depths for the uniform sediment were higher than those for the non-uniform sediments. Comparing the average scour volumes for all experiments of uniform and non-uniform sediments, the scour volume was found to be 40% greater in uniform sediments than in non-uniform sediments. Deposition volumes and deposition heights were also higher in the experiments with the uniform sediment, due to the armouring (Figure 3(a)–3(d)).

In some experiments with the non-uniform sediments, the relative scour depth decreased with increasing discharge (Figure 3(b)). In particular, in experiments with a 15 cm spur dike, although the scour depth increased in direct proportion to the discharge, the relative scour depth did not always increase with the flow depth. This effect was expected because of the complex mechanism of armouring.

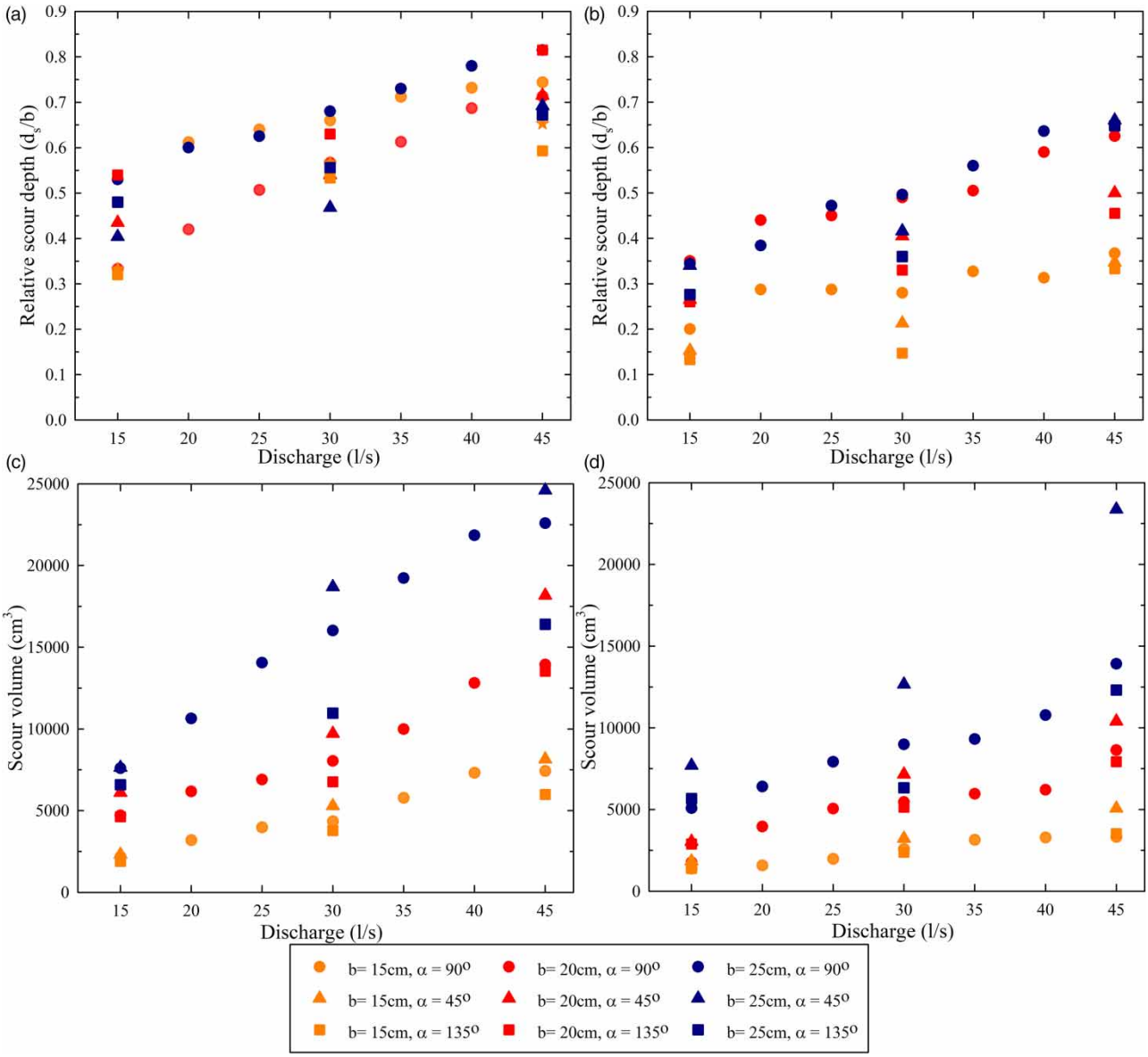

Figure 3 | Relative scour depths corresponding to discharges for (a) uniform and (b) non-uniform sediments; scour volumes corresponding to discharges for (c) uniform and (d) non-uniform sediments.

Effects of spur length and orientation angle

The experimental results indicate that the scour volume is directly related to the spur dike orientation angle. It is seen from Figure 3(c) and 3(d) that the 45° spur dike caused the highest turbulence. Accordingly, the scour volume was maximum at 45° spurs and minimum at 135° spurs, consistent with the results obtained by Kuhnle *et al.* (2002). They observed the highest scour volume at spur dikes directed upstream. In summary, as the spur orientation angle increased, the scour volume decreased for both uniform and non-uniform sediments at the same discharges.

Considering the scour depth results, the scour depth was maximum at 90° spurs (Figure 3(a) and 3(b)). Previous studies showed that the scour depth increases with a decrease in the spur dike orientation angle (Ahmad 1953; Zaghloul 1983; Melville & Coleman 2000). However, in some studies (Kandasamy 1985; Kwan 1988), the scour depth was found to be maximum at 90° spurs. Zhang *et al.* (2018) indicated that the scour depth and scour volume were maximum when the orientation angle was 90°. Clearly, previous results are not entirely consistent and sometimes contradictory. Therefore, when interpreting results related to the orientation angle, sediment gradation and spur dike geometry are vital.

The effect of orientation angle on scouring was different in the uniform and non-uniform sediments for 45° and 135° spurs. Contrary to expectations, 20 and 25 cm spurs at an angle of 45° had smaller scour depths than those at an angle of 135° in the uniform sediments. This shows that the spur length is more effective than the orientation angle for uniform sediments. In non-uniform sediments, the scour depths were minimum at 135° spurs, consistent with the scour volume results. This observation shows that the spur length and spur angle are interdependent parameters. In all the experiments, the effect of angle on scouring increased with increasing spur length.

As the spur length perpendicular to the flow increased, the contraction ratio (b/B) also increased. Accordingly, the cross-section of the flow became narrow, and the flow velocity increased. In general, the scour depth and scour volume increased with the spur length. The same trend was also observed for relative scour depths. However, as shown in Figure 3, the experimental results for 20 and 25 cm spurs show similar relative scour depths. This indicates that the influence of contraction ratio varies at a certain value and that the effect of the left-hand sidewall is non-negligible at high contraction ratios. To support this point, we carried out three more experiments with 10-cm-long spurs for the uniform sediments. The relative scour depths corresponding to the contraction ratios (four contraction ratios for uniform sediment and three contraction ratios for non-uniform sediment) are given in Figure 3.

Figure 4 shows that as the contraction ratio increases, the relative scour depth increases with a nonlinear relationship. However, for experiments with the highest contraction ratio ($b/B = 0.29$ for uniform sediments and $b/B = 0.36$ for non-uniform sediments), the relative scour depths tend to decrease. This decrement was also visible in bathymetric maps and scour depth measurements at sections having maximum scour depths. This change indicates that the opposite channel wall had a significant effect on the scour depth at a ratio of approximately $b/B = 0.29$ for uniform and $b/B = 0.36$ for non-uniform sediments.

Effects of discharge and flow depth

Although the flow intensity (V/V_c) was kept almost constant in all the experiments, the depth of scouring increased with increasing discharge and accordingly the flow depth (Figure 5). Evidently, the intensity of the above-mentioned vortex systems formed around the spur dike increased with the water depth. The water was not deep enough to form a horseshoe vortex or wake vortices in the experiments conducted with a low water depth. Figure 5 shows the sediment levels at the longitudinal sections, which intersect at the maximum scour depth coordinates. In addition, as shown in Figure 5, the maximum height of the deposited mounds shifts downstream, and the steepness of the mounds increases with increasing flow depth. This may indicate that the effect of the wake vortex also increased and that it moved farther as the flow depth increased.

Contour line maps

Scour hole contour maps were drawn for each experiment using the measurements taken by the laser meter. In general, as the discharge increased, scour holes generally got deeper (Figure 4). As the spur length increased, scour holes enlarged and got

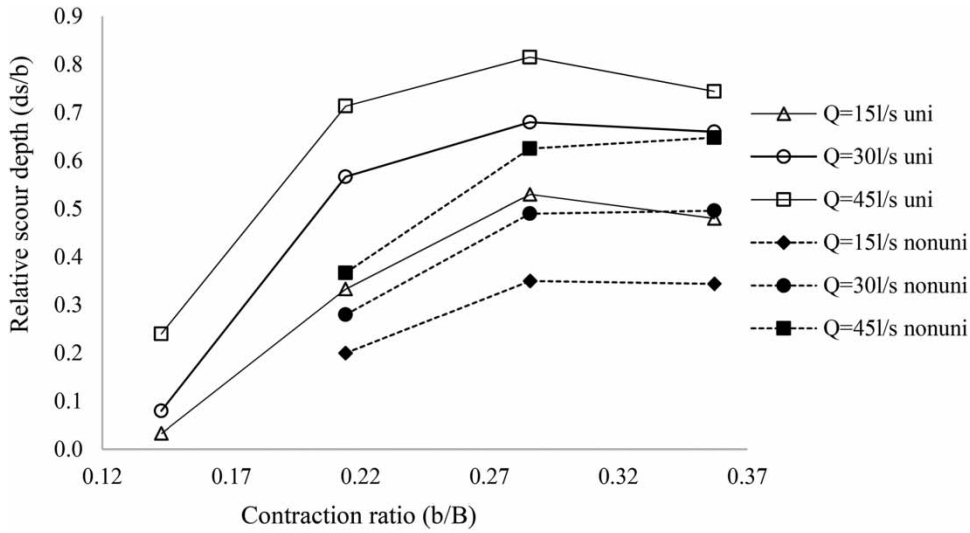

Figure 4 | Relative scour depths corresponding to contraction ratios for 90° spurs.

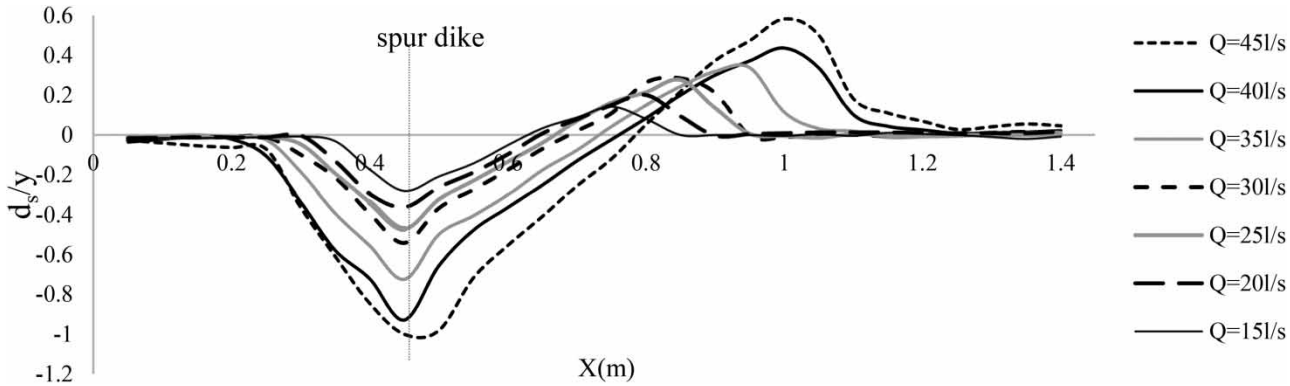

Figure 5 | Longitudinal section for experiments on uniform sediments ($b = 15$ cm, $\alpha = 90°$).

deeper, and the scour hole volumes increased. Maximum scour depths were observed at the nose of the spur dikes. The maximum scour depths and deposition mound heights are presented at the contour line indicator in Figures 6 and 7.

The bed deformation in the scouring area after the 30 l/s experiment is shown in Figure 5. The orientation angle of the spurs had important effects on the scouring geometry, depth and volume. The scour depths were maximum at the upstream side of the 45° spurs and downstream of the 135° spurs (Figure 6). The spurs having the highest scour volumes were the spurs angled at 45°, which caused the highest turbulence. The scour volumes were lowest for the 135° spurs. As the spur orientation angle increased, the scour volume decreased. In experiments with uniform base materials, the scour depth and mound height were higher than in the experiments with non-uniform base materials, while all the other conditions were kept constant. With the non-uniform sediment, the mound height downstream of the spur was 2 cm, whereas with the uniform base material, the mound height was approximately 8 cm (Figure 6). The scour areas downstream and upstream of the spur were evidently different. When $\alpha = 45°$, the scour area upstream was significantly greater than that downstream; when $\alpha = 135°$, the scour area of the spur dike downstream was larger.

In experiments with different angles, the shape of the scour was found to be different. The plane shape of the scour hole for 90° spurs was regular and nearly circular for all flow depths, whereas the downstream-oriented 135° spurs had an elliptical and slightly irregular shape. The scour hole reached the farthest distance in the flow direction for upstream-oriented spurs; however, the scour volume was the lowest (see Figures 3(c), 3(d) and 6).

The scour maps of the experiments with 35 l/s discharge and 90° spur orientation angle are shown in Figure 7. As mentioned earlier, the spur length had an important influence on the scour depth and volume. As the spur length increased, the zero-contour line (the scour area seen in the plan) extended and the contour lines became more frequent. As the spur length increased, the mound heights downstream of the spurs increased in both uniform and non-uniform sediments. The contraction effect shown in Figure 3 can also be seen in the contour graphs. Figure 7 shows that the zero-contour line for the 25 cm spur merges with the opposite channel wall. This wall effect was not observed in all the experiments with 10, 15, and 20 cm spur dikes.

Regression model

The relationship between the local scour depth and volume at a spur dike and its dependent parameters for this study can be written as:

$$d_s, \mathbb{V} = f(\rho, V, b, B, y, d_{50}, \alpha, \sigma_g, Fr)$$

where d_s is scour depth, $\mathbb{V}$ is scour volume, ρ is fluid density, V is flow velocity, b is spur dike length, y is the water depth, d_{50} is median grain diameter, α is spur dike angle and σ_g is geometric standard deviation. In this study, some parameters are assumed to be constant (such as channel slope, channel width, relative density of sediment etc.). The Buckingham π theorem can be used to generate dimensionless parameters (Buckingham 1914). The variables ρ, V and b are chosen as the recurring set. Finally, the following dimensionless terms can be derived for uniform and non-uniform sediments separately:

$$\frac{\mathbb{V}}{y^3} = f\left(\alpha, \frac{b}{B}, \frac{y}{b}, Fr\right)$$

$$\frac{d_s}{y} = f\left(\frac{b}{B}, \frac{y}{b}, Fr\right)$$

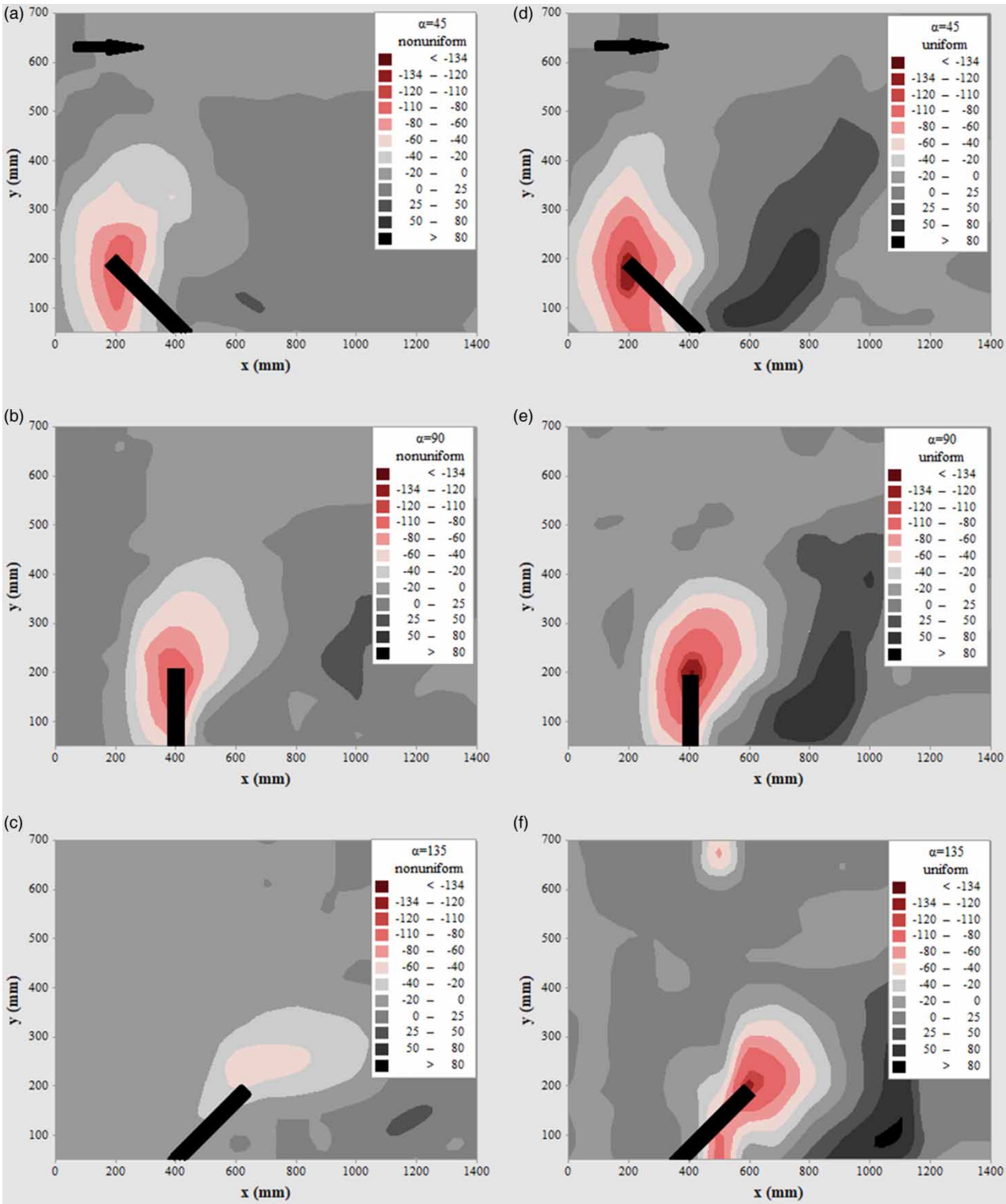

Figure 6 | Bathymetric maps of 30 l/s experiments for $b = 20$ cm; non-uniform sediments (a) $\alpha = 45°$, (b) $\alpha = 90°$, (c) $\alpha = 135°$; uniform sediments (d) $\alpha = 45°$, (e) $\alpha = 90°$, (f) $\alpha = 135°$.

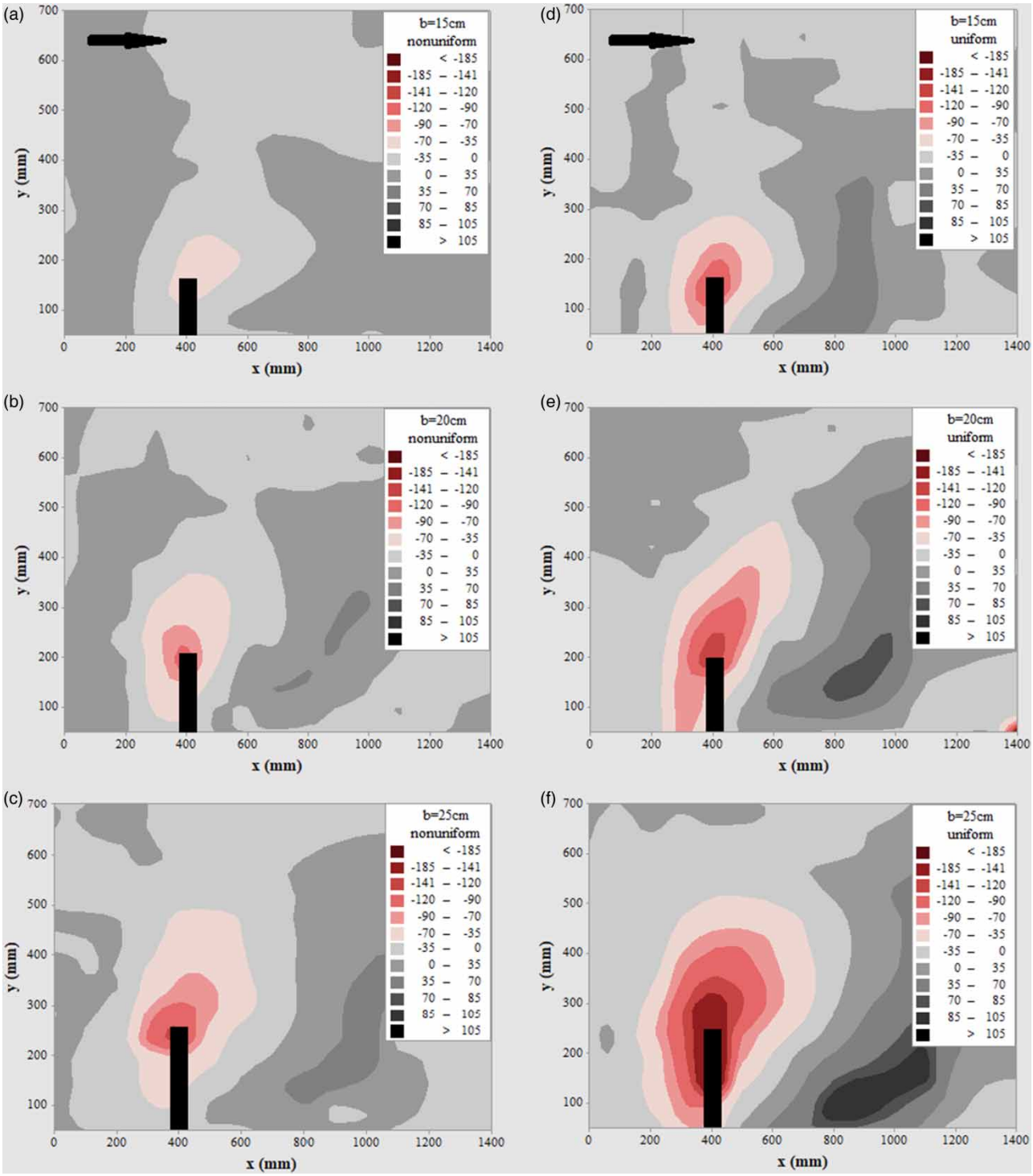

Figure 7 | Bathymetric maps of 35 l/s experiments for $\alpha = 90°$; non-uniform sediments (a) $b = 15$, (b) $b = 20$, (c) $b = 25$ cm; uniform sediments (d) $b = 15$, (e) $b = 20$, (f) $b = 25$ cm.

A stepwise regression analysis was performed using different dimensionless variables to evaluate the factors that influence the dependent variables, scour depth and scour volume. The stepwise regression procedure removes and adds the variables to the regression model for the purpose of identifying a useful subset of the variables (Ryan *et al.* 2012). In addition to the variables derived with the Buckingham π theorem, different dimensionless variables (d_{50}/y, d_{50}/b, V/V_{cr}, Re) were also added

while performing the stepwise regression analysis. Between the eight different dimensionless variables, the best model was the model with the Buckingham π variables.

Four equations were suggested, two for uniform sediments and two for non-uniform sediments, to determine the scour volume and depth. The constructed regression models with determination coefficients (R^2) can be expressed as follows:

Non-uniform sediment:

$$\frac{\mathbb{V}}{y^3} = 2.195 \left(\frac{b}{B}\right)^{0.743} \left(\frac{y}{b}\right)^{-1.823} \alpha^{-0.375} \quad R^2 = 0.97 \tag{1}$$

$$\frac{d_s}{y} = 42 \left(\frac{b}{B}\right)^{1.979} Fr^{1.175} \quad R^2 = 0.89 \tag{2}$$

Uniform sediment:

$$\frac{\mathbb{V}}{y^3} = 3.083 \left(\frac{b}{B}\right)^{0.659} \left(\frac{y}{b}\right)^{-1.735} \alpha^{-0.241} \quad R^2 = 0.97 \tag{3}$$

$$\frac{d_s}{y} = 72 \left(\frac{b}{B}\right)^{1.207} Fr^{1.787} \quad R^2 = 0.89 \tag{4}$$

In Equations (1) and (3), α is in radians. The equations are suitable for clear-water conditions and low Froude numbers. In all the equations, the scour depth and volume are mostly affected by the spur length and water depth. The parameter 'α' does not exist in the scour depth equations, since α did not evenly affect the scour depth and scour volume, as mentioned previously (in the 'Effects of Spur Length and Orientation Angle' subsection). Figure 8 shows the observation–estimation scatter diagrams of the regression models. Figure 8 shows that the results obtained using the equations are satisfactory with high R^2 values.

Determining the scour depth is challenging as it depends on many conditions; nevertheless, satisfactory estimates have been obtained in many previous studies. Equations have been suggested to estimate the scour depth near bridge piers, bridge abutments and spur dikes. We calculated the scour depths using these equations, with the variables of the present study. The equations that are applicable for clear-water scouring are listed in Table 2.

As shown in Figure 9, the equations given in the literature are comparable with our scour depth equation, despite the fact that the median particle diameters considered in these studies are not in the same range. However, the equations proposed by Dey & Barbhuiya (2005), Shen *et al.* (1969) and Melville (1997) overestimate the scour depth (Figure 9). Melville (1997) clearly stated that the suggested equation can be applied to local scouring and is restricted to bridge crossings where the contraction effects are insignificant. Dey & Barbhuiya (2005) reported the maximum contraction ratio value ($b/B = 0.13$). Because they investigated only local scouring around abutments, their equations might yield higher values than those proposed by Gill (1972) and the authors of the present study. As shown in Gill's (1972) equation, the contraction effect is an important parameter to calculate the scour depth. He addressed that one of the major parameters affecting the local erosion process is the contraction ratio. Because of the wide range of contraction ratios considered in the present study, the scour depths calculated with the previous equations considering the contraction effect overlap with the scour depths calculated with this study's model (Figure 9).

CONCLUSIONS

In this study, a series of experiments were conducted using spur dikes to investigate the effects of spur dike parameters on scouring under steady flow and clear-water conditions. The effect was described by measured scour depths and volumes. The data were analysed by conducting a dimensional analysis and relevant equations were suggested. The conclusions of this study are as follows:

1. The scour volume for uniform sediments was approximately 40% greater than that for non-uniform sediments, considering all the experimental results.
2. Increasing the orientation angle decreased the scour volume; however, it did not have a discernible influence on the scouring depth. The scour depths were maximum at 90° spurs whereas the scour volume was maximum at 45° spurs.

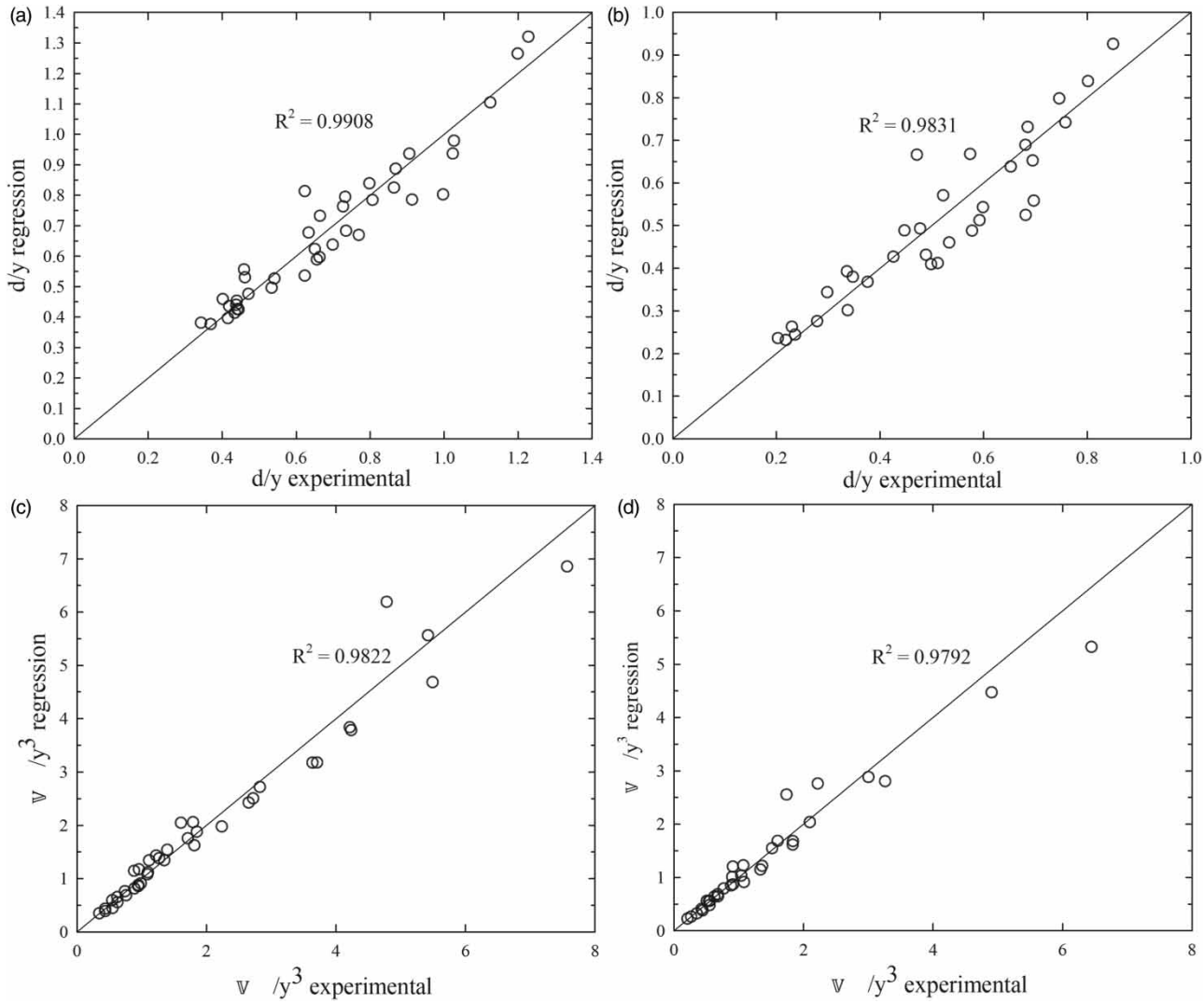

Figure 8 | Comparison of experimental measurements and estimations made using regression equations: scour depth for (a) uniform and (b) non-uniform sediments; scour volume for (c) uniform, (d) non-uniform sediments.

Table 2 | Equations for abutment or spur dike scour

Researcher	Equation	Conditions
Chitale (1962)	$\frac{d_s}{y} = -5.49\,Fr^2 + 6.65\,Fr - 0.51$	Clear-water – live-bed
Shen *et al.* (1969)	$\frac{d_s}{b} = 3.4\,Fr^{\frac{2}{3}}\,\frac{y^{\frac{1}{3}}}{b}$	Clear-water
Gill (1972)	$\frac{d_s + y}{y} = 8.375\,\frac{D_{50}}{y}^{0.25}\,\frac{b}{B-b}^{\frac{6}{7}}\,\frac{\tau_0}{\tau_{kr}}^{\frac{3}{7}}$	Clear-water
Melville (1997)	$d_s = K_{yw}K_I K_d K_s K_\alpha K_\sigma$	Clear-water – live-bed (no contraction)
Dey & Barbhuiya (2005)	$\frac{d_s}{b} = 7.281\,F_e^{0.314}\,\frac{y}{b}^{0.128}\,\frac{b}{D_{50}}^{-0.167}$	Clear-water (no contraction)

Where K_{yw} = depth size, K_I = flow intensity, K_d = sediment size, K_s = pier or abutment shape, K_g = pier or abutment alignment, and K_G = channel geometry. F_e is the excess abutment Froude number $(F_e = U - 0.5U_C/\sqrt{(\frac{\rho_S}{\rho} - 1)gl})$ for vertical wall abutments. Chitale (1962) employed different sands having mean diameters of 0.16 mm, 0.24 mm, 0.68 mm and 1.51 mm. Gill (1972) conducted experiments with sediments having median diameters of 0.1 mm and 0.9 mm. Shen *et al.* (1969) used available data in which the median diameter of the bed material was between 0.16 mm and 0.68 mm. Dey & Barbhuiya (2005) made a comprehensive experimental study, in which the median particle size ranged from 0.26 mm to 3.10 mm. Ettema (1980) indicated that when the ratio of the spur length to median diameter (b/d_{50}) is greater than 50, the scour depth is independent of the sediment size (Melville 1997). The b/d_{50} rate obtained in our study is between 82 and 208. Therefore, the suggested equations can be effectively used to predict the scour depth and scour volume for $b/d_{50} > 50$.

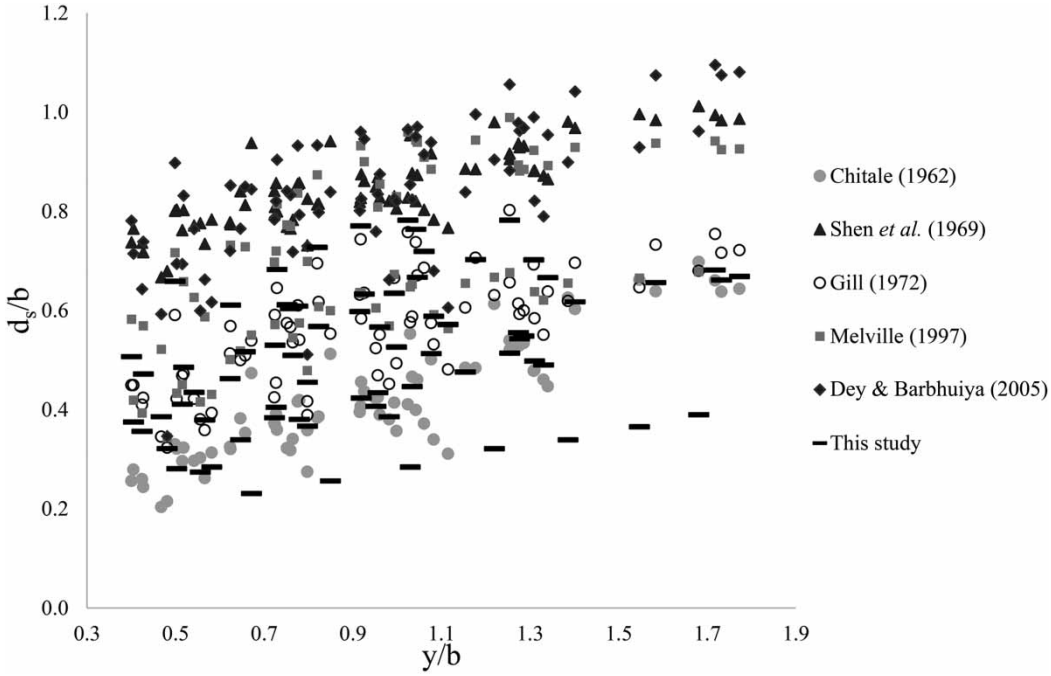

Figure 9 | Dimensionless scour depths calculated using equations from the literature.

3. The contraction effect played an active role when the contraction ratio (b/B) was greater than 0.29 for uniform sediments and 0.36 for non-uniform sediments with medium sand.
4. The dimensionless scour volume and scour depth for uniform and non-uniform sediments under clear-water conditions could be predicted by Equations (1)–(4).

In future research, additional experiments should be conducted to verify the present observations. Further experiments may be performed on a larger channel to investigate the contraction effect more efficiently. Finally, different sediment sizes can be selected to investigate the effect of geometric standard deviation.

ACKNOWLEDGEMENTS

This study was supported by Ege University Scientific Research Project Coordination with a project number of 15MUH033. Thanks also to the anonymous reviewers who offered valuable advice for the improvement of the manuscript.

DATA AVAILABILITY STATEMENT

All relevant data are included in the paper or its Supplementary Information.

REFERENCES

Ahmad, M. 1953 Experiments on design and behavior of spur dikes. In: *Proceedings of the Minnesota International Hydraulic Convention*. ASCE, New York, USA, pp. 145–159

Aksoy, A. O., Bombar, G., Arkis, T. & Guney, M. S. 2017 Study of the time-dependent clear water scour around circular bridge piers. *Journal of Hydrology and Hydromechanics* **65** (1), 26–34.

Ballio, F. & Orsi, E. 2001 Time evolution of scour around bridge abutments. *Water Engineering Research* **2**, 243–259.

Ballio, F., Teruzzi, A. & Radice, A. 2009 Constriction effects in clear water scour at abutments. *Journal of Hydraulic Engineering* **135** (2), 140–145.

Bestawy, A., Eltahawy, T., Alsaluli, A., Almaliki, A. & Alqurashi, M. 2020 Reduction of local scour around a bridge pier by using different shapes of pier slots and collars. *Water Supply* **20** (3), 1006–1015.

Breusers, H. N. C. & Raudkivi, A. J. 1991 *Scouring*. AA Balkema, Rotterdam, The Netherlands.

Briaud, J. L., Ting, F. C. K., Chen, H. C., Gudavalli, R., Perugu, S. & Wei, G. 1999 SRICOS: prediction of scour rate in cohesive soils at bridge piers. *Journal of Geotechnical and Geoenvironmental Engineering* **125**, 237–246.

Buckingham, E. 1914 On physically similar systems; illustrations of the use of dimensional equations. *Physical Review* **4** (4), 345–376.
Chiew, Y. M. 1984 *Local Scour at Bridge Piers*. PhD thesis, University of Auckland, Auckland, New Zealand.
Chitale, S. V. 1962 Discussion of 'Scour at bridge crossings'. *Transactions of the American Society of Civil Engineers* **127** (1), 191–196.
Dey, S. & Barbhuiya, A. K. 2005 Time variation of scour at abutments. *Journal of Hydraulic Engineering* **131** (1), 11–23.
Dey, S., Bose, S. K. & Sastry, G. L. 1995 Clear water scour at circular piers: a model. *Journal of Hydraulic Engineering* **121** (12), 869–876.
Dey, L., Barbhuiya, A. K. & Biswas, P. 2017 Experimental study on bank erosion and protection using submerged vane placed at an optimum angle in a 180° laboratory channel bend. *Geomorphology* **283**, 32–40.
Ettema, R. 1980 *Scour at Bridge Piers*. Transport Research Laboratory, Auckland, New Zealand.
Ezzeldin, M. M., Saafan, T. A., Rageh, O. S. & Nejm, L. M. 2007 Local scour around spur dikes. In: *Eleventh International Water Technology Conference*, Sharm el-Sheikh, Egypt, pp. 779–795.
Gill, M. A. 1972 Erosion of sand beds around spur dikes. *Journal of the Hydraulics Division* **98**, 1587–1602.
Gisonni, C. & Hager, W. H. 2008 Spur failure in river engineering. *Journal of Hydraulic Engineering* **134**, 135–145.
Kandasamy, J. K. 1985 *Local Scour at Skewed Abutments,* Report No. 375. University of Auckland, Auckland, New Zealand.
Karimi, N., Heidarnejad, M. & Masjedi, A. 2017 Scour depth at inclined bridge piers along a straight path: a laboratory study. *Engineering Science and Technology, an International Journal* **20** (4), 1302–1307.
Kirkil, G., Constantinescu, S. G. & Ettema, R. 2008 Coherent structures in the flow field around a circular cylinder with scour hole. *Journal of Hydraulic Engineering* **134** (5), 572–587.
Kothyari, U. C., Hager, W. H. & Oliveto, G. 2007 Generalized approach for clear-water scour at bridge foundation elements. *Journal of Hydraulic Engineering* **133** (11), 1229–1240.
Kuhnle, R. A., Alonso, C. V. & Shields, F. D. 1999 Geometry of scour holes associated with 90° spur dikes. *Journal of Hydraulic Engineering* **125** (9), 972–978.
Kuhnle, R. A., Alonso, C. V. & Shields Jr., F. D. 2002 Local scour associated with angled spur dikes. *Journal of Hydraulic Engineering* **128** (12), 1087–1093.
Kwan, T. F. 1988 *A Study of Abutment Scour,* Report No. 328. University of Auckland, Auckland, New Zealand.
Melville, B. W. 1997 Pier and abutment scour: integrated approach. *Journal of Hydraulic Engineering* **123** (2), 125–136.
Melville, B. W. & Coleman, S. E. 2000 *Bridge Scour*. Water Resources Publications, Highlands Ranch, CO, USA.
Melville, B. W. & Sutherland, A. J. 1988 Design method for local scour at bridge piers. *Journal of Hydraulic Engineering* **114** (10), 1210–1226.
Pagliara, S., Sagvand Hassanabadi, L. & Mahmoudi Kurdistani, S. 2015 Log-vane scour in clear water condition. *River Research and Applications* **31** (9), 1176–1182.
Pandey, M., Sharma, P. K., Ahmad, Z. & Singh, U. K. 2017 Evaluation of existing equations for temporal scour depth around circular bridge piers. *Environmental Fluid Mechanics* **17**, 981–995.
Pandey, M., Sharma, P. K., Ahmad, Z. & Singh, U. K. 2018 Experimental investigation of clear-water temporal scour variation around bridge pier in gravel. *Environmental Fluid Mechanics* **18**, 871–890.
Richardson, E. V. & Davis, S. R. 2001 *Evaluating Scour at Bridges*, 4th edn. Federal Highway Administration, Washington, DC, USA.
Ryan, B. F., Joiner, B. L. & Cryer, J. D. 2012 *MINITAB Handbook: Updated for Release 16*. Cengage Learning, Boston, MA, USA.
Shen, H. W., Schneider, V. R. & Karaki, S. 1969 Local scour around bridge piers. *Journal of the Hydraulics Division* **95** (6), 1919–1940.
Sheppard, D. M. & Miller, W. 2006 Live-bed local pier scour experiments. *Journal of Hydraulic Engineering* **132** (7), 635–642.
Singh, R. K., Pandey, M., Pu, J. H., Pasupuleti, S. & Villuri, V. G. K. 2020 Experimental study of clear-water contraction scour. *Water Supply* **20** (3), 943–952.
Uddin, M. N. & Rahman, M. M. 2012 Flow and erosion at a bend in the braided Jamuna River. *International Journal of Sediment Research* **27** (4), 498–509.
USACE 1989 *Fundamental Procedure for Developing a Physical Model Using Micro Model Methodology*. USACE, St Louis District, MO, USA.
Yilmaz, M., Yanmaz, A. M. & Koken, M. 2017 Clear-water scour evolution at dual bridge piers. *Canadian Journal of Civil Engineering* **44** (4), 298–307.
Yuan, C., Melville, B. W. & Adams, K. N. 2017 Scour at wind turbine tripod foundation under steady flow. *Ocean Engineering* **141**, 277–282.
Zaghloul, N. A. 1983 Local scour around spur-dikes. *Journal of Hydrology* **60**, 123–140.
Zhang, H. 2005 *Study on Flow and Bed Evolution in Channels with Spur Dykes*. PhD thesis, Department of Civil Engineering, Kyoto University, Kyoto, Japan.
Zhang, H., Nakagawa, H., Kawaike, K. & Baba, Y. 2009 Experiment and simulation of turbulent flow in local scour around a spur dyke. *International Journal of Sediment Research* **24** (1), 33–45.
Zhang, L., Wang, H., Zhang, X., Wang, B. & Chen, J. 2018 The 3-D morphology evolution of spur dike scour under clear-water scour conditions. *Water* **10** (11), 1583.

First received 19 July 2021; accepted in revised form 2 November 2021. Available online 16 November 2021